



Faraday Discussions

Amplified spontaneous emission from liquid crystalline phase: anisotropic property and active modulation

Journal:	<i>Faraday Discussions</i>
Manuscript ID	FD-ART-06-2023-000122
Article Type:	Paper
Date Submitted by the Author:	18-Jun-2023
Complete List of Authors:	Tsutsui, Yusuke; Kyoto University, Molecular Engineering; JST, Sakurai, Tsuneaki; Kyoto Institute of Technology, Faculty of Molecular Chemistry and Engineering Seki, Shu; Kyoto University, Molecular Engineering

SCHOLARONE™
Manuscripts

ARTICLE

Amplified spontaneous emission from liquid crystalline phase: anisotropic property and active modulation

Yusuke Tsutsui,^{*a,b} Tsuneaki Sakurai^c and Shu Seki^{*a}

Received 00th January 20xx,

Accepted 00th January 20xx

DOI: 10.1039/x0xx00000x

Amplified spontaneous emission (ASE) is considered to be a primary indication of optical gain in active media without an external resonator. Molecular materials with ASE is expected to be one of the suitable light sources for specific application such as optical coherent tomography owing to their low coherence and flexible tunability. Concentration quenching of emissive excited states has been a critical issue to boost quantum efficiency of molecular materials in their condensed phases. The rod-like design of molecule with excited state intramolecular proton transfer (ESIPT) has been demonstrated to overcome this issue in highly-concentrated molecularly doped system, as represented by C4alkyne-HBT (2-(4-(1-hexynyl)-2-hydroxyphenyl)-benzothiazole). We designed ESIPT molecule-doped liquid crystalline (LC) system for optical amplification via ASE regime with its wide tunability of emission intensity. Detailed ASE behaviour and optical gain of a LC blend of C4alkyne-HBT and 4-pentyl-4'-cyano biphenyl (5CB) was evaluated to afford maximum optical gain of 16.5 cm⁻¹ with the estimated ASE threshold of optical pump at 0.6–0.7 mJ cm⁻². Although most of ASE studies focus on the homogeneous solutions, solids, or crystalline states, ASE from soft-flexible LC phase is quite limited and advantageous for the design of an external optical resonator/cavity structure. Optical excitation parallel and perpendicular to the director resulted in the strong modulation of ASE. By using the profit of LC phase, ASE was actively modulated under the external electric field by the reorientation of molecular dipole moment.

Introduction

Considering the structural relaxation in photoexcited organic molecules, total relaxation processes can be inherently regarded as a four-level system which provides an ideal platform for lasing application of the molecules. Historically, organic dyes have often employed as lasing media, especially to keep broad band emission in spectral range required for the generation of ultrashort pulse.^{1–4} They have also been used as convenient tunable laser sources in broad spectral range thanks to plenty of rotational and vibrational states of the dyes upon photoexcitation.^{5,6} The major advantages of organic molecule/dyes are in the diverse range of chemical structures designed for demanded optical properties such as wavelength, bandwidth, quantum yield, and lifetime.

Amplified spontaneous emission (ASE) is a process of light amplification of spontaneous emission accumulated with stimulated emission. The gain of the amplification process is recognized as a prime indication of laser action in the media without external cavity structure. ASE is expected as an excellent candidate for light source due to its low coherence and tunability for optical coherent tomography (OCT).^{7,8} ASE from randomly distributed organic dyes was well implemented as dye laser system with solutions of the molecules.^{9–11} Recently, laser emission or ASE have been reported from solid or crystalline states of various organic materials such as oligo-thiophenes,^{12,13} rylenes,¹⁴ spirobifluorene,^{15–17} and styrylbenzene-family.^{16,18–23}

Although most of ASE studies started from solution states, shifting into solid or crystalline states of the media, ASE from liquid crystalline (LC) phase is less studied so far.^{24,25} Liquid crystalline phase is especially advantageous to have a fast response to the external stimuli such as electric field and temperature due to its fluidity and oriented dipole moment. This controllable orientation of molecules in LC phase is expected to realize dynamic manipulation of optical gain and ASE processes by using itself as a lasing media, which cannot be achieved in solution nor crystalline states. Choices of the guest molecules in the LC media enable the wide-range modulation of emission property such as lasing wavelength and non-linear threshold. The key demand for the guest molecules is to realize an interplay of high emissive nature and compatibility against host LC phases without aggregation under heavily doped concentrations.

^a Department of Molecular Engineering, Graduate School of Engineering, Kyoto University, Nishikyo-ku, Kyoto 615-8510, Japan

^b JST-PRESTO, Honcho 4-1-8, Kawaguchi, Saitama 332-0012, Japan

^c Faculty of Molecular Chemistry and Engineering, Kyoto Institute of Technology, Matsugasaki, Sakyo-ku, Kyoto 606-8585, Japan

Electronic Supplementary Information (ESI) available: [details of any supplementary information available should be included here]. See DOI: 10.1039/x0xx00000x

A critical issue of the doped system has been concentration quenching from self-absorption, energy transfer, and aggregation of guest molecules.^{26,27} To reduce self-absorption, one of the approaches is to reduce the overlap of absorption and emission spectra, with the design of *e.g.* anti-Kasha emission and large structural relaxation at excited state. We focused on the excited state intramolecular proton transfer (ESIPT) process where the proton transfer occurs from donor to acceptor moiety at its excited state to realize large structural and energy relaxation. This is originated from the reversed free energy of different isomers in electronic ground and excited states. Various structural frameworks are reported to exhibit ESIPT with presenting ASE behaviour in solid or crystalline states.^{24,28–32} Based on the representative ESIPT molecular motif of 2-(2-hydroxyphenyl)-benzothiazole (HBT), we designed rod-like molecule with high aspect ratio: 2-(4-(1-hexynyl)-2-hydroxyphenyl)-benzothiazole (C4alkyne-HBT) showing relatively high fluorescence quantum yield in various media.³³ In this work, the detailed optical property of C4alkyne-HBT in liquid crystalline media: 4-pentyl-4'-cyano biphenyl (5CB) have been studied as well as demonstrating anisotropic emission property and dynamic control of the emission and optical gain.

Results and discussion

Optical property of C4alkyne-HBT

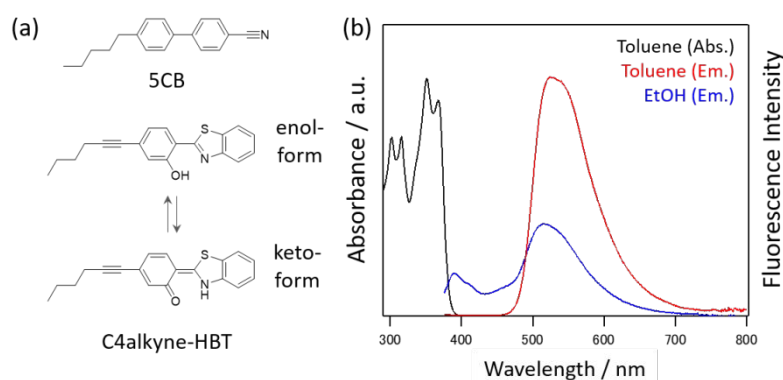


Fig. 1 (a) Chemical structures of C4alkyne-HBT and 5CB. For C4alkyne-HBT, isomerization process is also shown. (b) Absorption and fluorescence spectra of C4alkyne-HBT in toluene and ethanol. Excitation wavelength was set to 365 nm.

C4alkyne-HBT was synthesized based on our previous paper³³. This molecule exhibits *keto-enol* isomerism where the proton on a hydroxyl group moves to the nitrogen of a benzothiazole ring with bond alternation (Fig. 1(a)). At its electronic ground state, the enol form is more stable than its *keto*-form; the stability reverses at the first singlet excited state, driving isomerism from *enol** to *keto**-forms. This ESIPT behaviour induces large structural relaxation at excited state making its fluorescence observed at far longer wavelength. It is shown in the Fig. 1(b) that the absorption (351 nm) and fluorescence (525 nm) in toluene were actually well separated with the Stokes shift of 1.17 eV ($= 9440 \text{ cm}^{-1}$ estimated from their maxima). The overlap of absorption and fluorescence spectra is effectively suppressed to avoid concentration quenching due to the self-absorption and energy transfer. The ESIPT process is largely affected by the surrounding media due to their different polarity, viscosity, and orientation to the emitter molecule through the modulation in both static and dynamic energy landscape. When the solvent was replaced to more polar ethanol, the new fluorescence band appeared due to the contribution of the *enol** and anion forms^{34,35}. The proton donating ability of hydroxyl group in ethanol competes the ESIPT process of HBT to partially inhibits the ESIPT, resulting in the observation of *enol** emission at 380–420 nm. The anion emission may be overlapped at around 450 nm as a minor shoulder. The anion species is generated at the excited state due to the hydrogen bonding between proton of the phenol group in HBT and oxygen in an ethanol molecule.

C4alkyne-HBT itself only shows the crystal to isotropic liquid phase transition at $\sim 100^\circ\text{C}$ without liquid crystalline phase, but is highly soluble to conventional room temperature liquid crystal 5CB up to 14wt% ($\sim 12 \text{ mol}\%$ or 0.46 M) without aggregation owing to its alkynyl group³³. The LC blend samples were prepared by mixing C4alkyne-HBT into 5CB with the ratio of 1 and 14wt% to observe the effect of doping level.

ASE property of C4alkyne-HBT and 5CB blend samples

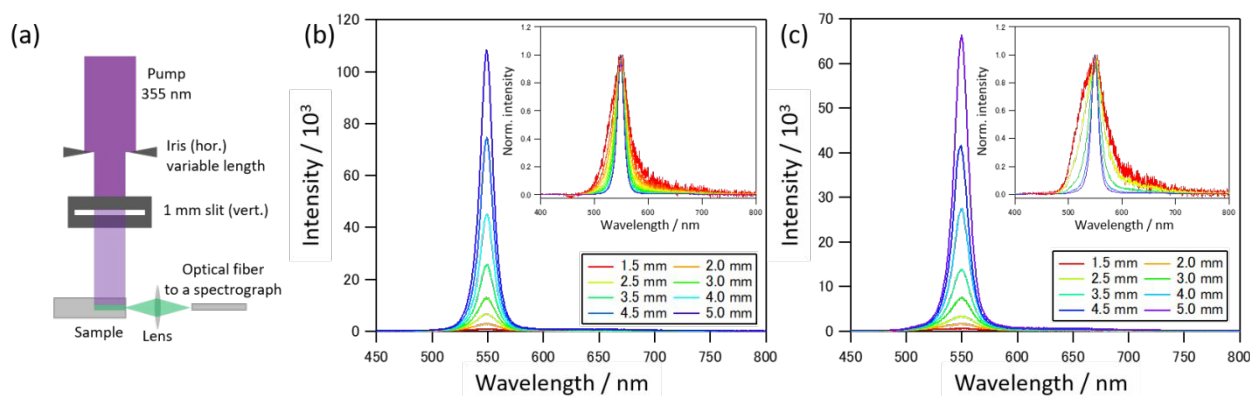


Fig. 2. (a) Experimental setup to collect variable length emission spectra from the LC blends. Emission spectra of C4alkyne-HBT/5CB blend with mixing ratio of (b) 1wt% and (c) 14wt%. Pump beam size was adjusted from 1.5 to 5 mm with the pump fluence of 2 mJ cm^{-2} . Insets show normalized emission spectra.

The fluorescence quantum yield of C4alkyne-HBT is relatively high as $\Phi = 0.32$ in 5CB, remaining unchanged under doping level at 1wt%, 5wt%, and 14wt%. This is suggestive of homogeneous distribution of C4alkyne-HBT in the LC media and the negligible concentration quenching in the present LC blend (LC host-guest system). ESIPT process in HBT is known to be quite fast in the sub-picosecond regime,^{36–38} and fluorescence rate is relatively slow as $k_r = 1.1 \times 10^8 \text{ s}^{-1}$ for C4alkyne-HBT in 5CB. This prompt tautomerization populates the higher level effectively to realize inverted population, making C4alkyne-HBT as a fascinating platform to model a four level emitter. We thus expected to observe ASE from this LC blend under high excitation density. Emission spectra of LC samples at high pump fluence were obtained with the experimental setup shown in Fig. 2(a). The samples were excited by nanosecond UV pulses (355 nm) with a rectangular shape where the short side was fixed at 1 mm and the long side was varied in 1.5–5 mm with keeping the identical excitation density. The emission from the sample was collected along the long side of the excited area. In this configuration, photons, generated by spontaneous emission, travel along the longer path to reach the optical fiber with interacting with the excited molecules. Thus, the optical gain could be estimated by varying the optical length.^{39–41} The obtained emission spectra of LC blends at variable length are shown in Fig. 2(b) and (c). These spectra showed sharp peak at around 548 nm, and the intensity increases monotonically with enlarging pump area. Since the peak is close to the emission maximum of *keto* tautomer, the emission is mostly contributed after the successful ESIPT process in 5CB (Fig. S1). Normalized emission spectra are also shown in the insets of Fig. 2(b) and (c). In both cases, the full-width at half maximum (FWHM) decreases monotonically to present narrower emission at longer optical path, suggesting the existence of optical gain in these media with the pump fluence of 2 mJ cm^{-2} . Although this fluence is the largest value used in our experiment, similar ASE behaviour was observed with decreased fluences as shown in the following.

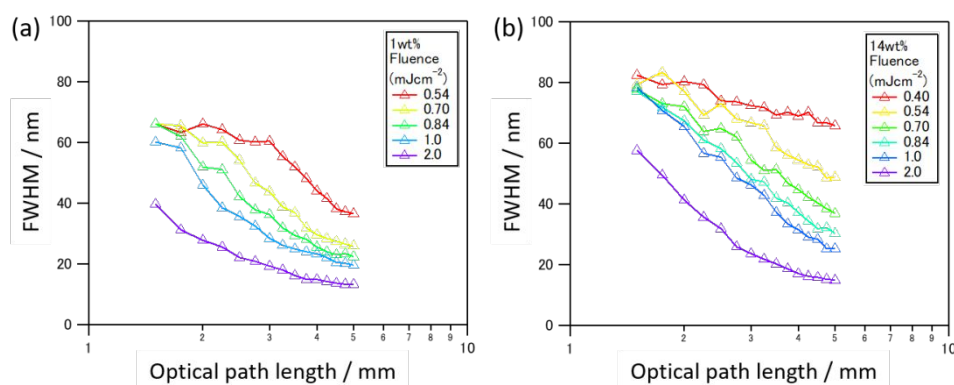


Fig. 3. Full-width at half-maximum values of the emission spectra from (a) 1wt% and (b) 14wt% samples under the series of pump fluence.

FWHM values are plotted against pump fluence in Fig. 3. Increasing both in optical path length and excitation fluence reduced FWHM values. However, FWHM is larger in 14wt% under the same condition. For example, at the fluence of 2 mJ cm^{-2} , FWHM decreased to similar values of 13–14 nm for the blend ratio of both 1wt% and 14wt%, but the maximum FWHM value at the lower optical path was 1.5 times larger in 14wt%. This is also the case of dependence on excitation fluence, suggesting the larger ASE threshold for 14wt%. The original FWHM observed with low enough excitation fluence was $\sim 86 \text{ nm}$ in 5CB (Fig. S3). The ASE threshold, derived from a mid-point of FWHM between 13 and 86 nm, was approximately estimated to be ~ 0.6 (0.7) mJ cm^{-2} for the 1(14)wt% sample.

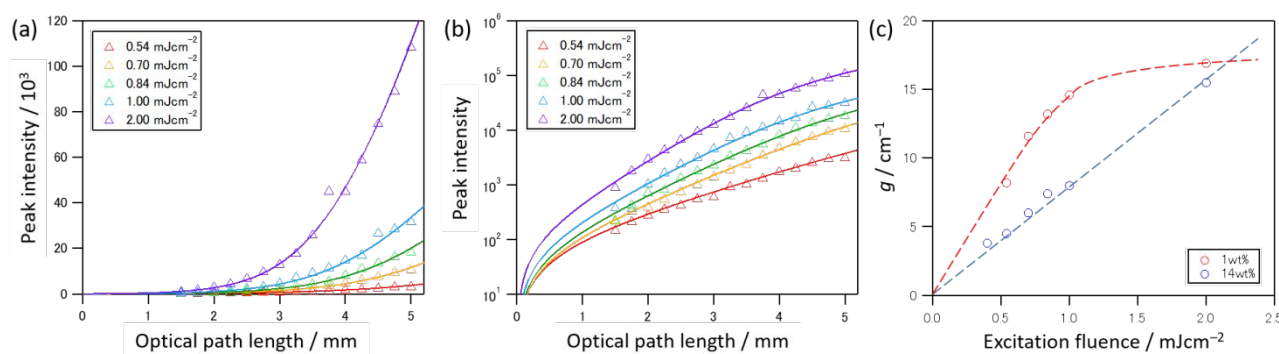


Fig. 4. Pump beam size dependence of integrated emission intensity from C4alkyne-HBT(1wt%)/5CB blend plotted in (a) linear and (b) semi-logarithmic scale. Pump energy was varied from 27 to 100 μ J and shown with fitted profiles. (c) Optical gain of C4alkyne-HBT/5CB with concentration of 1 (red) and 14wt% (blue). The dotted lines are the guides for eyes.

The intensity of the emission spectra at peak wavelength (~ 548 nm) was plotted against the length of the long side in rectangular pump beam (Fig. 4(a)). Since the pump area was varied with keeping the excitation density as same value, the emission intensity is expected to show linear relationship on the pump area (*i.e.* longer length of pump area) in the linear system. However, non-linear behaviour was apparently observed in Fig. 4(a), indicating the appearance of ASE. The modulation in pump fluence from 0.54 to 2.0 mJ cm^{-2} resulted in similar non-linear behavior. This relationship was well represented by one-pathway amplifier equation with α and β as fitting parameters

$$gL = \alpha I + \ln(\beta I + 1), \quad (1)$$

where g , L , and I are optical gain, longer side length of pump beam, and emission intensity, respectively^{39–41}. From the fitting, optical gain for 1wt% blend was estimated to be $g = 8.2\text{--}16.9 \text{ cm}^{-1}$ depending on the excitation fluence. This value is competitive to those of the typical high performance fluorescent dyes such as coumarin family ($7\text{--}50 \text{ cm}^{-1}$)⁴², rhodamine ($\sim 10 \text{ cm}^{-1}$)⁴³, diethylthiatricarbocyanine iodide (DTTC) ($\sim 2.5 \text{ cm}^{-1}$)⁴⁴, and perylene family ($\sim 4\text{--}53 \text{ cm}^{-1}$)^{45,46}. The emission intensity in the 14wt% medium was similarly analysed to lead an estimate of optical gain as $3.8\text{--}15.5 \text{ cm}^{-1}$, depending largely on the fluence (Fig. S2). Since the ESPT process separates far apart the absorption and fluorescence bands, optical loss originated from reabsorption of the emitted photon would be negligible in these devices.

To examine optical gain difference in detail, fluence dependence of optical gain is plotted in Fig. 4(c). At lower excitation density, the optical gain of 1wt% blend surpassed that of 14wt%. This would be considered as a loss of excited energy via intermolecular energy transfer under high concentration, or the excited state transient absorption. The optical gain of 1wt% tends to saturate at higher excitation density, but it still holds to increase in the 14wt% device with a linear relationship. The reason for the saturation in 1wt% could be considered in several ways. (I): Due to the less number of molecules, optical absorption would be saturated. The number of photons at the highest excitation density of 2 mJ cm^{-2} is equivalent to 1.8×10^{14} photons in the pump area ($1 \times 5 \text{ mm}$). The number of emitter molecules in the volume along optical path ($1 \text{ mm} \times 5 \text{ mm} \times 5 \mu\text{m}$) is estimated to be 5×10^{14} and 7×10^{15} molecules for 1 and 14wt%, respectively. The number of molecules reaches up to the comparable order to the number of photons in 1wt% at highest excitation density. Since the number of excited molecules tend to be saturated in 1wt% blend, optical gain may be saturated as well. To clarify this hypothesis, the transmittance at 355 nm was measured with various excitation density. However, it resulted in the constant value of $\sim 15\%$ up to the highest excitation, suggesting that no saturation of excited states presumed even in the 1wt% device. (II): The depth of the optical penetration is different for these devices. Considering the extinction coefficient of $\sim 3 \times 10^4 \text{ M}^{-1} \text{ cm}^{-1}$ at 355 nm and an order parameter $S_{\text{abs}} = 0.46$, the optical penetration depth is estimated to be 1.8 and 0.13 μm for 1wt% and 14wt%, respectively. Since the emission could only be collected at a limited angle, if the system exceeds ASE threshold well enough, ASE may occur effectively for different direction as well, which saturates the optical gain at specific angle. The 1wt% device results in higher possibility in this situation than 14wt% device due to its larger penetration depth, hence the lower geometric anisotropic ratio.

Polarization dependence of amplified spontaneous emission

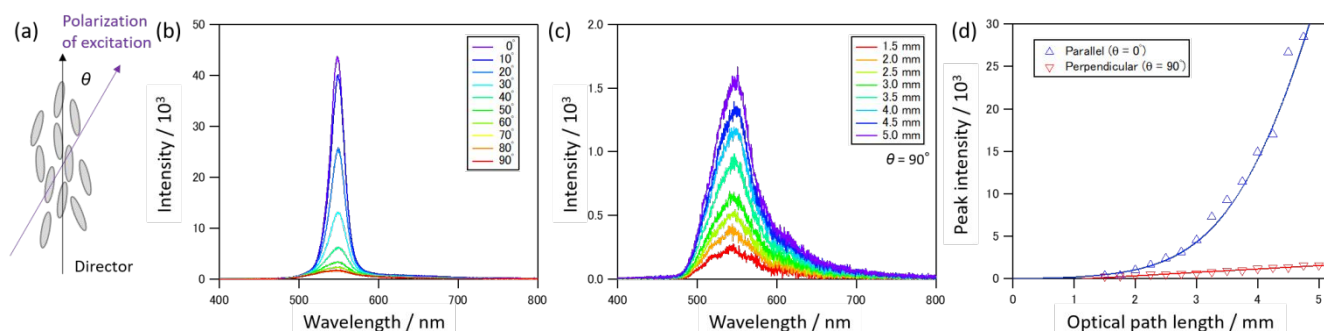


Fig. 5 Anisotropic emission measurement for 1wt% C4alkyne-HBT/5CB blend sample with the fixed pump fluence of 1 mJ cm^{-2} . (a) Definition of the rotation angle ϑ . (b) Dependence of emission spectra on the polarization of the pump. Optical path length was fixed at 5 mm. (c) Emission spectra at perpendicular configuration ($\vartheta = 90^\circ$). Optical path length was adjusted from 1.5 to 5 mm. (d) Comparison of emission intensity under parallel and perpendicular excitation.

Liquid crystal is the molecularly oriented mesophase without the periodicity of the centre of mass. The orientational axis, called as a director, is normally taken along the long molecular axis, and we followed this convention as shown in Fig. 5(a). Considering the profit of liquid crystalline phase, orientational or anisotropic property of ASE would be of interests for the design of external stimuli-sensitive devices. The polarization of the excitation was freely rotated with a half wave plate with the excitation density of 1 mJ cm^{-2} , which is well above the ASE threshold at parallel excitation ($\vartheta = 0^\circ$) to the director. As shown in Fig. 5(b), mismatching in excitation polarization from the director resulted in the monotonic decrease in the emission intensity. In addition, emission spectra broadened at larger angles, indicating strong suppression of ASE (Fig. S3). This is also confirmed by the variable optical length method discussed in the previous section. Fig 5(c) shows the dependence of emission spectra on optical path length (pump area) at perpendicular excitation ($\vartheta = 90^\circ$), presenting no significant change in the spectral shape nor broadness of the spectra. Compared to the parallel excitation, emission intensity at perpendicular configuration only resulted in linear dependence on pump area (Fig. 5 (d)), indicating negligible ASE in this configuration. These results indicate that the LC blend of C4alkyne-HBT (emitter) and 5CB (LC host) can be utilized as ASE emitter and modulator, which would potentially be applicable as an active lasing media.

Active control of amplified spontaneous emission

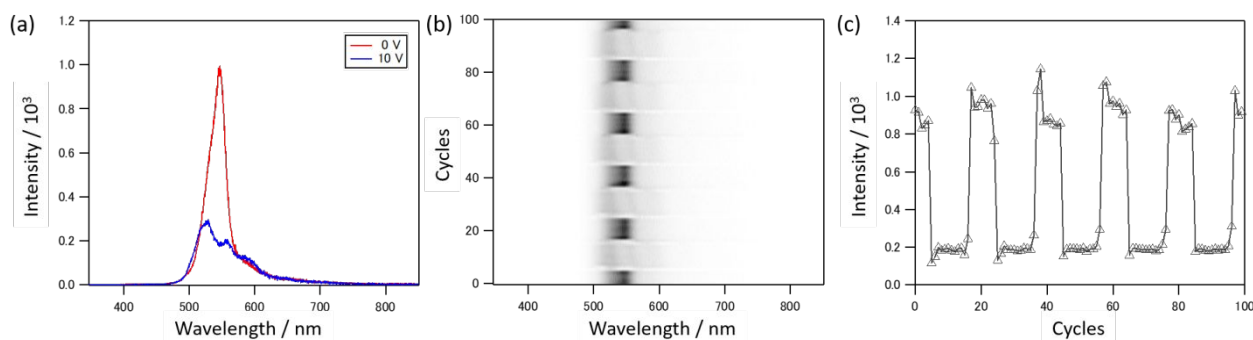


Fig. 6 (a) Emission Spectra of 1wt% C4alkyne-HBT/5CB blend under the application of the voltage. (b) Two dimensional map of emission spectra under the application of square wave voltage (0.5 Hz, $10 V_{p-p}$). (c) The time trace of emission intensity at 548 nm.

Here, using the orientational property to the external electric field, active control of ASE was demonstrated in liquid crystalline phase: the advantage of LC media. The excitation density was set to 1 mJ cm^{-2} , which is well above the ASE threshold. When the voltage bias of 10 V was applied to the LC cell, significant suppression of ASE was observed as shown in Fig. 6(a). The molecules are reorientated by the electric field due to their dipole moment so that the director of the molecules become collinear to the propagation vector of the excitation pulse, resulted in the strong suppression in optical absorption under the voltage bias. Since the net density of excited state reduces, the ASE pumping threshold dramatically increases under the application of the voltage, resulting in the significant suppression in the optical gain. To show the switching ability of ASE clearly, 0.5 Hz square wave voltage of 0-10 V_{p-p} was applied to the LC cell. As shown in the Fig 6(b), the ASE behaviour could be dynamically controlled. By taking the emission intensity at 548 nm, the time trace shows quick response to the external electric field (Fig6(c)). These results are originated from the profit of the LC phase, which will open the new avenue for the active control of optical gain and further development for active optical materials and devices.

Conclusions

Optical property of HBT-based emitter C4alkyne-HBT was evaluated and analysed in detail with variable doping level to 5CB. ASE behaviour was clearly observed under the high excitation fluence with the narrowing of the spectra down to 13–14 nm and the non-linear increase in the emission intensity. ASE threshold was estimated to be 0.6–0.7 mJ cm⁻² from the half-point of the spectral FWHM. Optical gain coefficient was also estimated as 8.2–16.9 and 3.8–15.5 cm⁻¹ for 1wt% and 14wt% blends, respectively, which is in the similar order as the typical organic laser dyes. In addition, anisotropic excitation response and active control of ASE was observed thanks to the orientational property of the LC phase.

Experimental

Materials and sample preparation

C4alkyne-HBT was synthesized and purified based on the previous procedure³³. Liquid crystal 5CB was purchased from Tokyo Chemical Industry Co. Ltd. and used as received. C4alkyne-HBT was blended with 5CB with the concentration of 1 or 14wt% at 50 °C under argon atmosphere, cooled down to room temperature, and loaded into a 5- μ m thick LC cell purchased from EHC Co., Japan. The inner surface of the glasses of the cell are coated with patterned ITO and covered with the anti-parallel-directed polyimide rubbing.

Conventional absorption and fluorescence measurements

Electronic absorption spectra were recorded on a JASCO V-730 spectrometer. Fluorescence spectra were measured on a JASCO FP-8500 fluorescence spectrophotometer. Absolute fluorescence quantum yields (Φ) were evaluated on this spectrometer with a JASCO ILF-835 fluorescence integrate sphere unit.

Amplified spontaneous emission measurements

The sample cells were excited from the front surface perpendicularly with the third harmonics of Nd:YAG nanosecond laser (355 nm, 10 Hz, pulse width of 7–9 ns for fundamental, LOTIS-TII LS-2131M). Excitation beam profile was variably adjusted with a manual slit to be a rectangular of 1 mm x 1.5–5.0 mm. The emission was collected from the edge of the sample with a lens and an optical fibre to be detected with a spectrograph and EMCCD (Andor, Kymera 328i and Newton DU970P-BVF). Square wave voltage (10 V_{p-p}, 0.5 Hz) was applied to the ITO cell by a function generator (Tektronix AFG1062) for the orientation control of the liquid crystalline phase and emission spectra were acquired with 10 Hz.

Author Contributions

Y. T. performed the optical experiments, analysis, and wrote the manuscript. T. S. synthesized fluorescence materials, prepared the LC devices, measured absorption/fluorescence spectra, and edited the manuscript. S. S. guided, reviewed, and edited the manuscript.

Conflicts of interest

There are no conflicts to declare.

Acknowledgements

This work was supported by JST, PRESTO Grant Number JPMJPR21Q5 and a Grant-in-Aid for Scientific Research (nos. 22H00314, 20H05862 and 20H05867).

References

- 1 W. H. Glenn, M. J. Brienza and A. J. DeMaria, *Appl. Phys. Lett.*, 1968, **12**, 54–56.
- 2 B. H. Soffer and J. W. Linn, *Journal of Applied Physics*, 1968, **39**, 5859–5860.
- 3 O. G. Peterson, S. A. Tuccio and B. B. Snavely, *Appl. Phys. Lett.*, 1970, **17**, 245–247.
- 4 R. L. Fork, B. I. Greene and C. V. Shank, *Appl. Phys. Lett.*, 1981, **38**, 671–672.
- 5 M. Maeda and Y. Miyazoe, *Jpn. J. Appl. Phys.*, 1972, **11**, 692–698.
- 6 B. H. Soffer and B. B. McFarland, *Appl. Phys. Lett.*, 1967, **10**, 266–267.
- 7 N. Feng, M. Lu, S. Sun, A. Liu, X. Chai, X. Bai, J. Hu and Y. Zhang, *Laser Photonics Rev.*, 2023, 2200908.
- 8 D. Huang, E. A. Swanson, C. P. Lin, J. S. Schuman, W. G. Stinson, W. Chang, M. R. Hee, T. Flotte, K. Gregory, C. A. Puliafito and J. G. Fujimoto, *Science*, 1991, **254**, 1178–1181.
- 9 M. Terada and Y. Ohba, *Jpn. J. Appl. Phys.*, 1983, **22**, 1392.
- 10 G. Marowsky, F. K. Tittel, W. L. Wilson and E. Frenkel, *Appl. Opt.*, 1980, **19**, 138.

- 11 U. Ganiel, A. Hardy, G. Neumann and D. Treves, *IEEE J. Quantum Electron.*, 1975, **11**, 881–892.
- 12 M. Polo, A. Camposo, S. Tavazzi, L. Raimondo, P. Spearman, A. Papagni, R. Cingolani and D. Pisignano, *Appl. Phys. Lett.*, 2008, **92**, 083311.
- 13 V. Navarro-Fuster, E. M. Calzado, M. G. Ramirez, P. G. Boj, J. T. Henssler, A. J. Matzger, V. Hernández, J. T. López Navarrete and M. A. Díaz-García, *J. Mater. Chem.*, 2009, **19**, 6556.
- 14 E. M. Calzado, J. M. Villalvilla, P. G. Boj, J. A. Quintana, R. Gómez, J. L. Segura and M. A. Díaz-García, *J. Phys. Chem. C*, 2007, **111**, 13595–13605.
- 15 N. Johansson, J. Salbeck, J. Bauer, F. Weissörtel, P. Bröms, A. Andersson and W. R. Salaneck, *Synth. Metal.*, 1999, **101**, 405–408.
- 16 H. Nakanotani, S. Akiyama, D. Ohnishi, M. Moriwake, M. Yahiro, T. Yoshihara, S. Tobita and C. Adachi, *Adv. Funct. Mater.*, 2007, **17**, 2328–2335.
- 17 M. Inoue, T. Matsushima and C. Adachi, *Appl. Phys. Lett.*, 2016, **108**, 133302.
- 18 F. Hide, M. A. Díaz-García, B. J. Schwartz, M. R. Andersson, Q. Pei and A. J. Heeger, *Science*, 1996, **273**, 1833–1836.
- 19 M. Fakis, I. Polyzos, G. Tsigaridas, V. Giannetas, P. Persephonis, I. Spiliopoulos and J. Mikroyannidis, *Opt. Mater.*, 2004, **27**, 503–507.
- 20 W. Xie, F. Li, H. Wang, Z. Xie, F. Shen, Y. Ma, W. Lu, D. Zhang and D. Ma, *Appl. Opt.*, 2007, **46**, 4431.
- 21 R. Kabe, H. Nakanotani, T. Sakanoue, M. Yahiro and C. Adachi, *Adv. Mater.*, 2009, **21**, 4034–4038.
- 22 M. Mamada, H. Nakanotani and C. Adachi, *Mater. Adv.*, 2021, **2**, 3906–3914.
- 23 H. Mochizuki, *Bull. Chem. Soc. Jpn.*, 2022, **95**, 1039–1041.
- 24 M. Durko-Maciąg, G. Ulrich, D. Jacquemin, J. Mysliwiec and J. Massue, *Phys. Chem. Chem. Phys.*, 2023, **25**, 15085–15098.
- 25 Y. Tsutsui, W. Zhang, S. Ghosh, T. Sakurai, H. Yoshida, M. Ozaki, T. Akutagawa and S. Seki, *Adv. Opt. Mater.*, 2020, **8**, 1902158.
- 26 J. Gierschner, J. Shi, B. Milián-Medina, D. Roca-Sanjuán, S. Varghese and S. Park, *Adv. Opt. Mater.*, 2021, **9**, 2002251.
- 27 C. V. Bindhu, S. S. Harilal, G. K. Varier, R. C. Issac, V. P. N. Nampoory and C. P. G. Vallabhan, *J. Phys. D: Appl. Phys.*, 1996, **29**, 1074–1079.
- 28 C.-C. Yan, X.-D. Wang and L.-S. Liao, *ACS Photonics*, 2020, **7**, 1355–1366.
- 29 J. Massue, A. Felouat, P. M. Vérité, D. Jacquemin, K. Cypriach, M. Durko, L. Sznitko, J. Mysliwiec and G. Ulrich, *Phys. Chem. Chem. Phys.*, 2018, **20**, 19958–19963.
- 30 K. Sakai, T. Tsuzuki, Y. Itoh, M. Ichikawa and Y. Taniguchi, *Appl. Phys. Lett.*, 2005, **86**, 081103.
- 31 X. Cheng, Y. Zhang, S. Han, F. Li, H. Zhang and Y. Wang, *Chem. Eur. J.*, 2016, **22**, 4899–4903.
- 32 S. Park, J. E. Kwon, S.-Y. Park, O.-H. Kwon, J. K. Kim, S.-J. Yoon, J. W. Chung, D. R. Whang, S. K. Park, D. K. Lee, D.-J. Jang, J. Gierschner and S. Y. Park, *Adv. Opt. Mater.*, 2017, **5**, 1700353.
- 33 W. Zhang, S. Suzuki, S. Cho, G. Watanabe, H. Yoshida, T. Sakurai, M. Aotani, Y. Tsutsui, M. Ozaki and S. Seki, *Langmuir*, 2019, **35**, 14031–14041.
- 34 J. Cheng, D. Liu, W. Li, L. Bao and K. Han, *J. Phys. Chem. C*, 2015, **119**, 4242–4251.
- 35 K. Sakai, T. Ishikawa and T. Akutagawa, *J. Mater. Chem. C*, 2013, **1**, 7866.
- 36 P. F. Barbara, P. K. Walsh and L. E. Brus, *J. Phys. Chem.*, 1989, **93**, 29–34.
- 37 J. L. Herek, S. Pedersen and L. Bañares, *J. Chem. Phys.*, 1992, **97**, 9046.
- 38 Th. Arthen-Engeland, T. Bultmann, N. P. Ernstring, M. A. Rodriguez and W. Thiel, *Chem. Phys.*, 1992, **163**, 43–53.
- 39 W. Heudorfer, G. Marowsky and F. K. Tittel, *Z. Naturforsch. A*, 1978, **33**, 1062–1068.
- 40 K. L. Shaklee, R. E. Nahory and R. F. Leheny, *J. Lumin.*, 1973, **7**, 284–309.
- 41 K. L. Shaklee and R. F. Leheny, *Appl. Phys. Lett.*, 1971, **18**, 475–477.
- 42 U. Itoh, M. Takakusa, T. Moriya and S. Saito, *Jpn. J. Appl. Phys.*, 1977, **16**, 1059–1060.
- 43 C. V. Shank, A. Dienes and W. T. Silfvast, *Appl. Phys. Lett.*, 1970, **17**, 307–309.
- 44 P. G. Gillard, N. D. Foltz and C. W. Cho, *Appl. Phys. Lett.*, 1973, **23**, 325–327.
- 45 H. Manaa, *J. Alloys Compd.*, 2005, **393**, 219–222.
- 46 M. R. Kaysir, S. Fleming, R. W. MacQueen, T. W. Schmidt and A. Argyros, *Appl. Opt.*, 2016, **55**, 178.